

# Kinetics of Hydrogen Diffusion in $\text{LaNi}_{5-x}\text{Sn}_x$ Alloys

*B. V. Ratnakumar*

*Electrochemical Technologies Group,  
Jet Propulsion Laboratory, Pasadena, CA 91109  
and*

*A. Hightower, C. Witham, R. C. Bowman, and B. Fultz  
Division of Engineering and Applied Science  
California Institute of Technology, Pasadena, CA 91125*

## ABSTRACT

Solid-state diffusion of hydrogen in metal hydride (MH) alloys is recognized as the rate determining step in the discharge of MH alloys in alkaline Ni-MH rechargeable cells. In our pursuit of new ternary solutes in  $\text{LaNi}_5$  for extended cyclic lifetimes, we have observed noticeable improvement in the cycle life with small substitutions of Sn and Ce for Ni. Furthermore, these substituents also facilitate enhanced charge transfer kinetics for hydriding-dehydriding process. In this paper, we report our studies on the kinetics of hydrogen diffusion in  $\text{LaNi}_{5-x}\text{Sn}_x$  alloys by electrochemical pulse techniques, chronoamperometry and chronocoulometry. The measured diffusion coefficients for hydrogen in MH alloys are of order of  $10^{-9} \text{ cm}^2/\text{s}$ .

## 1.0 INTRODUCTION

The durability of  $\text{LaNi}_5$ -based electrodes during electrochemical cycling, is generally improved by a partial substitution of La or Ni with suitable solutes. Various additives such as Nd,<sup>1</sup> Ti,<sup>2</sup> Zr<sup>3</sup> and Ce<sup>4</sup> for La and Co,<sup>1</sup> Mn, Al<sup>5</sup> and Si<sup>1</sup> for Ni have been found to be successful substituents for lowering the absorption plateau pressures and/or improving the cycle life. Sakai et al.<sup>5</sup> evaluated several substituents for Ni but found that the improvement in the cycle life is unfortunately accompanied by a decrease in the hydrogen absorption capacity, long activation, or slow kinetics. The use of Sn as a partial substituent for Ni in  $\text{LaNi}_5$ , on the other hand, was found to reduce the absorption plateau pressure and minimize the hysteresis, while retaining most of the high absorption capacity of the binary alloy.<sup>6</sup> Furthermore, the Sn substituent was found to result in a 20-fold increase in the cyclic lifetime in thermal cycling<sup>7</sup> and a charge-discharge cycle life comparable to a multi-component, misch metal based alloy.<sup>8</sup> Additionally, the kinetics of hydrogen absorption-desorption appear to be more facile upon Sn substitution, indicating that favorable surface conditions are prevalent on these alloys.<sup>9</sup> Similar beneficial effects were also realized with Ce substituent.<sup>10</sup>

Electrochemical hydriding-dehydriding reaction of MII alloy contains a series of steps. For example, the charge transfer reaction produces adsorbed atomic hydrogen ( $H_{ad}$ ) and OH on the electrode surface (Volmer process). The adsorbed hydrogen either diffuses through the surface layer and grain boundaries into the bulk of the alloy to form the hydride, or combines with adjacent adsorbed hydrogen atom to form molecular hydrogen (Tafel process) and thus hydrogen evolution. The performance of the metal hydride electrode is determined by the kinetics of the process occurring at the electrode/electrolyte interface as well as of hydrogen transport within the bulk of the alloy. The charge transfer process is the rate determining step for electrodes containing small particles, while the hydrogen diffusion dominates for larger particles.<sup>11</sup>

Reliable values for hydrogen diffusion coefficients in  $LaNi_5$  hydride phases have been difficult to obtain due to complex microscopic diffusion processes in crystal structures where hydrogen simultaneously occupies several distinct types of interstitial sites.<sup>12,13</sup> Furthermore, various physical properties of activated  $LaNi_5H_x$  powders often impeded analyses and interpretations of commonly employed techniques such as nuclear magnetic resonance (NMR) and quasi elastic neutron scattering (QNS). Performing a critical assessment of NMR and QNS methods to characterize hydrogen diffusion in  $\beta$ - $LaNi_5H_x$  when  $x > 6$ , Richter et al.<sup>12</sup> concluded that the imp.-range diffusion coefficient at 300 K is in the range of  $1 - 5 \times 10^{-8} \text{ cm}^2/\text{s}$ . Züchner et al.<sup>14</sup> applied current pulse electrochemical method on single crystal  $\alpha$ - $LaNi_5H_x$  with  $x < 0.07$  to obtain anisotropic diffusion coefficient of  $2 - 3 \times 10^{-8} \text{ cm}^2/\text{s}$  at 298 K. Apparently, there is not a large difference in hydrogen diffusion behavior between these two phases even though the hydrogen contents vary considerably.

There have been relatively few studies<sup>12</sup> on the effect of substitutional alloying on hydrogen diffusion in the  $AB_5$  hydrides. Using NMR methods, Bowman et al.<sup>15</sup> showed that Al substitution greatly decreased hydrogen motion in the  $\beta$ - $LaNi_{5-y}Al_yH_x$  with an accompanying increase in activation energy. Zheng et al.<sup>16</sup> obtained with electrochemical methods a room temperature diffusion coefficient of  $3 \times 10^{-11} \text{ cm}^2/\text{s}$  for an  $LaNi_{4.25}Al_{0.75}$  hydride electrode which was below the value of  $7 \times 10^{-10} \text{ cm}^2/\text{s}$  reported for a  $LaNi_4Cu$  electrode by van Rijswijk.<sup>11</sup> More recently, Zheng et al.<sup>17</sup> used a constant current discharge technique to derive the hydrogen diffusion constant of  $7 \times 10^{-11} \text{ cm}^2/\text{s}$  for a  $LaNi_{4.27}Sn_{0.24}$  electrode. Ilisc-type electrodes made with  $MmNi_{4.2}Al_{0.5}M_{0.3}$  ( $M = Cr, Mn, Fe, Co, Ni$ ) were used by Iwakura, et al.<sup>18</sup> to evaluate hydrogen diffusion coefficients in the  $\alpha$ -phase by the electrochemical potential step method. The diffusion constants measured at 303 K ranged between  $1.6 \times 10^{-8} \text{ cm}^2/\text{s}$  to  $3.2 \times 10^{-8} \text{ cm}^2/\text{s}$ . It should be noted (not the hydrogen diffusion coefficients deduced using electrochemical methods on alloy

powders are smaller by one to two orders of magnitude than values obtained from NMR, QNS, or electrochemical measurements on bulk samples.<sup>14, 15</sup>

In this work, we studied the transport kinetics of hydrogen in  $\text{LaNi}_{5-x}\text{Sn}_x$  alloys by electrochemical pulse techniques, i.e., chronoamperometry and chronocoulometry. Sn substitution results in improved interfacial conditions for electrochemical hydriding-dehydriding processes and in lower absorption pressures due to enlarged lattice volume. It is interesting to see if these features, especially the latter, also lead to enhanced transport of hydrogen within the bulk of the alloy. The results from these studies, combined with the extensive electrochemical and structural characterization already performed on  $\text{LaNi}_{5-x}\text{Sn}_x$  alloys, will help us better understand the role of the ternary solute on hydrogen diffusion.

## 2.0 EXPERIMENTAL

$\text{LaNi}_{5-x}\text{Sn}_x$  alloys were prepared by induction-melting and were subsequently annealed.<sup>9</sup> The annealed ingots were subjected to five hydrogen absorption/desorption cycles to activate the alloys. Metal hydride disk electrodes were prepared by filling the BAS (Bioanalytical Systems) disk electrodes with mixture of MI I powders (with 19% Ni and 5% Pt, PTFE), of equal quantities in each case to ensure equal surface area ( $0.07\text{ cm}^2$ ), density ( $5.6\text{ g/cm}^3$ ), and porosity in all the electrodes. A NiOOH electrode formed the counter-electrode, and a  $\text{Hg/HgO}$  ( $0.098\text{ V vs. SHE}$ ) with a Luggin capillary served as the reference electrode in a three-electrode, flooded cell with 31w% KOH electrolyte.

The experiments include constant current charges at  $40\text{ mA/cm}^2$  ( $\sim 20\text{ mA/g}$ ) to a capacity corresponding to  $400\text{ mAh/g}$ , potentiodynamic polarization curves for estimating diffusion limiting currents, constant-current discharges at  $64\text{ mA/cm}^2$  ( $33\text{ mA/g}$ ) to  $-0.5\text{ V vs. Hg/HgO}$  for calculating the absorbed hydrogen concentration in the alloy and chronoamperometric and chronocoulometric transient measurements for determining the diffusion coefficients. The polarization experiments were carried out with an EG&G 273 Potentiostat / Galvanostat using 352 corrosion software. Chronocoulometric response was monitored with a Nicolet storage oscilloscope. All the measurements were made at ambient temperature, which was  $25^\circ \pm 2^\circ\text{ C}$ .

It may be difficult to distinguish the hydriding and hydrogen evolution processes electrochemically. In a potentiodynamic polarization, for example, a smooth, almost unnoticeable, transition occurs from the hydride formation to the hydrogen evolution.<sup>9</sup> The concurrent hydrogen evolution thus induces uncertainties in the analysis of cathodic polarization data, due to reduced current efficiency and changing surface conditions. In order to alleviate such uncertainties, the present studies are restricted to the anodic regime, both for transient and steady-state experiments. Besides, the slow diffusing

species during discharge are undoubtedly hydrogen within the bulk of the alloy, whereas in the charging process, hydroxyl ions in the electrolyte phase could move more sluggishly, depending on the porosity and tortuosity of the electrode.<sup>17</sup>

### 3.0 RESULTS

#### 3.1 Steady State Measurements

##### 3.1.1 Potentiodynamic Polarization - Limiting currents

Figure 1 shows the steady state polarization curves of  $\text{LaNi}_{5-x}\text{Sn}_x$  alloys with different Sn contents ( $x$  from 0 to 0.5) at a slow scan rate (0.5 mV/s) approximating steady state conditions. The polarization curves show strong interference of mass transfer processes on the charge transfer kinetics, as evident from the current being invariant with an increase in the overpotential. At high overpotentials,  $> 400$  mV, the discharge reaction is limited by the rate of transport of hydrogen within the bulk of the alloy. The corresponding current, termed diffusion limiting current and estimated from Fig. 1 increases upon Sn substitution and decreases later at  $x \geq 0.2$  (Fig. 2). The low limiting current of the binary alloy is caused by the difficulty associated with its charging in a partially-sealed cell. The limiting currents of the Sn-substituted alloys are  $\sim 500$  mA/g as reported earlier for  $\text{LaNi}_5$ .

##### 3.1.2 Discharge Characteristics

In order to obtain the value of hydrogen concentration required for calculating the diffusion coefficients from the transient response below, the electrodes were discharged after a prior, complete charge. Fig. 3 shows the discharge curves of  $\text{LaNi}_{5-x}\text{Sn}_x$  alloys. The discrepancy in the electrochemical capacity in these alloys is partially due to the differences in their absorption plateau pressures.<sup>9</sup> MH alloys with high plateau pressures ( $> 1$  atm.) are not efficiently charged in the open cell adopted for the present studies. At high Sn contents, on the other hand, the discharge kinetics are relatively sluggish. The capacity is thus maximum with a Sn content of 0.2-0.3.

It should be realized that the degree of hydriding is such that the MH alloy exists in the two phase region, i.e., in the  $\alpha$  and  $\beta$  form. The measured diffusion coefficients therefore represent a weighted average value of  $\alpha$  and  $\beta$  phase hydrides.

## 3.2 Transient Measurements

### 3.2.1 Chronoamperometry

The transient methods involve the application of a potentiostatic pulse (corresponding to mass transfer regime identified in the steady-state experiment) to the electrode and monitoring amperometric and coulometric responses. From the dependence of diffusion current and coulombic charge on time, it is possible to obtain values for the diffusion coefficients by applying appropriate diffusion equations. The boundary conditions applicable to the present case for the outward diffusion of hydrogen within the bulk of the alloy are i) uniform initial concentration, i.e., at  $t = 0$ , the concentration of hydrogen is the same at any distance from the interface,  $x$ , ii) at  $t > 0$ , the concentration at large  $x$  approaches the bulk concentration and iii) the interfacial hydrogen concentration is zero at  $t > 0$ , after the potential step. Assuming semi-infinite linear diffusion conditions, the instantaneous current in the diffusion-limited regime may be expressed by Cottrell's equation<sup>19</sup> as

$$i = \frac{n F A D_H^{1/2} C^*}{\pi^{1/2} t^{1/2}} \quad (1)$$

where  $i$  is the instantaneous current at time  $t$ ,  $D_H$  is the diffusion coefficient of hydrogen,  $C^*$  is the bulk concentration of the diffusing species,  $A$  is the area of the electrode and  $F$  is the Faraday constant. The concentration  $C^*$  is obtained from the electrochemical discharge capacities, using the geometric volume of the electrode (Fig. 3, Table 1).

Fig. 4 shows the chronoamperometric curves of  $\text{LaNi}_{5-x}\text{Sn}_x$  alloys after applying a potentiostatic pulse of +400 mV vs. OCV, which corresponds to the diffusion-controlled regime. The corresponding plots between the current and  $t^{-1/2}$  recast from Fig. 4 are shown in Fig. 5. From the slope of these curves in Fig. 5 and bulk concentrations of hydrogen estimated above, the diffusion coefficients of hydrogen in  $\text{LaNi}_{5-x}\text{Sn}_x$  alloys were calculated (Table 1). The diffusion coefficients thus calculated are  $6.69 \times 10^{-9}$ ,  $8.38 \times 10^{-9}$ ,  $7.53 \times 10^{-9}$ ,  $9.36 \times 10^{-9}$  and  $2 \times 10^{-8} \text{ cm}^2/\text{s}$  for Sn contents of 0.1, 0.2, 0.3, 0.4 and 0.5, respectively (Fig. 6, Table 1).

### 3.2.2. Chronocoulometry

Here also, the electrode potential is shifted to a sufficiently positive value (for oxidation) to enforce diffusion-limited conditions. The coulometric output from the potentiostat is recorded as a function of time. The coulometric response may be described by the Cottrell equation in an integral form<sup>19</sup> such as

$$Q = \frac{2nFA D_H^{1/2} C^* t^{1/2}}{z^{1/2}} \quad (2)$$

where Q is the cumulative charge passed at any instant, t. A plot of Q vs.  $t^{1/2}$  is thus linear, the slope of which yields the diffusion coefficient.

Chronoamperometric curves were obtained for  $\text{LaNi}_{5-x}\text{Sn}_x$  alloys at a potentiostatic pulse corresponding to an anodic perturbation of 400 mV (Fig. 7). The corresponding plots between coulombic charge and  $t^{1/2}$  recast from Fig. 7 are shown in Fig. 8. From the slope of these curves in Fig. 8 and the bulk concentrations of absorbed hydrogen, the diffusion coefficients for hydrogen in  $\text{LaNi}_{5-x}\text{Sn}_x$  alloys were calculated (Table 1). The diffusion coefficients thus obtained are  $3.49 \times 10^{-9}$ ,  $3.86 \times 10^{-9}$  and  $3.77 \times 10^{-9}$   $\text{cm}^2/\text{s}$  for Sn contents of 0.2, 0.3 and 0.4, respectively (Fig. 6, Table 1).

#### 4.0 CONCLUSIONS

The diffusion coefficients of hydrogen in  $\text{LaNi}_{5-x}\text{Sn}_x$ , obtained from the amperometric and coulometric outputs upon a potential pulse corresponding to the diffusion limiting conditions, are in close agreement with each other, suggesting that the analyses and the assumptions involved are reasonable. These values of the diffusion coefficients are marginally lower than those obtained from NMR and QNS techniques, but clearly larger than the values of Zheng et al, obtained from constant-current discharges.

Finally, with increasing Sn content in  $\text{LaNi}_{5-x}\text{Sn}_x$  alloys, the diffusion of hydrogen is not hindered, whereas some sluggishness was observed earlier in the charge transfer kinetics. On the other hand, the diffusion of hydrogen seems to be enhanced marginally upon the substitution of Sn for Ni. This may possibly be related to the increased unit cell volume upon partial substitution of Ni with Sn.

#### 5.0 ACKNOWLEDGMENTS

This work was carried out at the Jet Propulsion Laboratory under contract with the National Aeronautics and Space Administration and at the California Institute of Technology under funding by the DOE grant D1-1-(i03-941iR14493).

## REFERENCES

1. G. G. Willems, *Philips J. Res.*, **39** (Suppl. D), 1 (1984); J. G. (i. Willems and K. H. J. Buschow, *J. Less Common Metals*, **129**, 13(1987).
2. T. Sakai, H. Miyamura, N. Kuriyama, A. Kato, K. Oguru, and H. Ishikawa, *J. Less Common Metals*, **159**, 127 (1990).
3. T. Sakai, H. Miyamura, N. Kuriyama, A. Kato, K. Oguru, and H. Ishikawa, *J. Electrochem. Soc.*, **137**, 795 (1990).
4. T. Sakai, T. Iizama, H. Miyamura, N. Kuriyama, A. Kato, and H. Ishikawa, *J. Less Common Metals*, **172-174**, 1175(1991).
5. T. Sakai, K. Oguru, H. Miyamura, N. Kuriyama, A. Kato, and H. Ishikawa, *J. Less Common Metals*, **161**, 193 (1990).
6. M. H. Mendelsohn, D. M. Gruen, and A. E. Dwight, *Mat. Res. Bull.*, **13**, 1221 (1979).
7. R. C. Bowman, Jr., C. H. Luo, C. C. Ahn, C. K. Witham, and B. Fultz, *J. Alloys and Compounds*, **217**, 185 (1995).
8. B. V. Ratnakumar, G. Halpert, C. Witham and B. Fultz, *J. Electrochem. Soc.*, **141**, I, 89(1994); *Proc. ECS Symp. Hydrogen Batteries.*, 94-27, 57(1994).
9. B. V. Ratnakumar, C. Witham, R. C. Bowman, Jr., A. Hightower, and B. Fultz, *J. Electrochem. Soc.* **143**, 2578 (1996).
10. C. Witham, B. V. Ratnakumar, R. C. Bowman, Jr., A. Hightower, and B. Fultz, *J. Electrochem. Soc.* **144**, 1, 204 (1996).
11. M. H. J. VanRijswijk, in *Hydrides for Energy Storage*, Ed., A. F. Anderssen and A. J. Maeland, p. 261, Pergamon, Oxford (1978).
12. D. Richter, R. Hempelmann, and R. C. Bowman, Jr., in *Hydrogen in Intermetallic Compounds II*, Ed L. Schlapbach (Springer-Verlag, Berlin, 1992) p. 97.
13. C. Schönfeld, R. Hempelmann, D. Richter, T. Springer, A. J. Dianoux, J. J. Rush, T. J. Udovic, and S. M. Bennington, *Phys. Rev. B* **50**, 853 (1994).
14. H. Züchner, T. Rauf, and R. Hempelmann, *J. Less-Common Met.* **172-174**, 611 (1991).
15. R. C. Bowman, Jr., D. M. Gruen, and M. H. Mendelsohn, *Solid State Commun.* **32**, 101 (1979).
16. G. Zheng, B. N. Popov, and R. E. White, *J. Electrochem. Soc.* **142**, 2695 (1995).
17. G. Zheng, B. N. Popov, and R. E. White, *J. Electrochem. Soc.* **143**, 834 (1996).
18. C. Iwakura, T. Oura, H. Inoue, M. Matsuoka, Y. Yamamoto, *J. Electroanal. Chem.* **398**, 37 (1995).
19. A. J. Bard and L. R. Faulkner, *Electrochemical Methods; Fundamentals and Applications*, John Wiley & Sons, Inc., New York (1980).

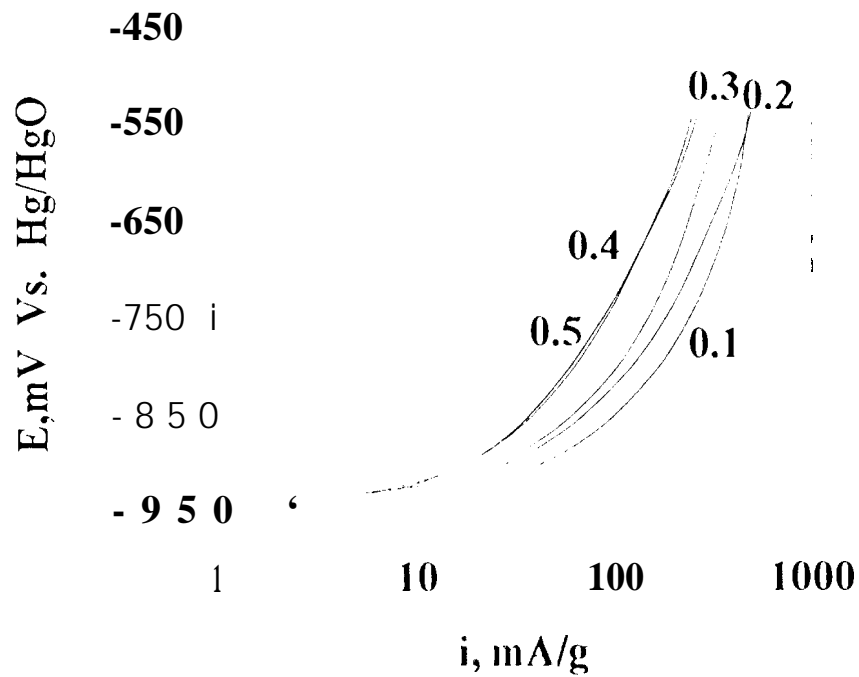


Fig. 1: Potentiodynamic polarization curves of  $\text{LaNi}_{5-x}\text{Sn}_x$  alloys, illustrating diffusion-limited behavior

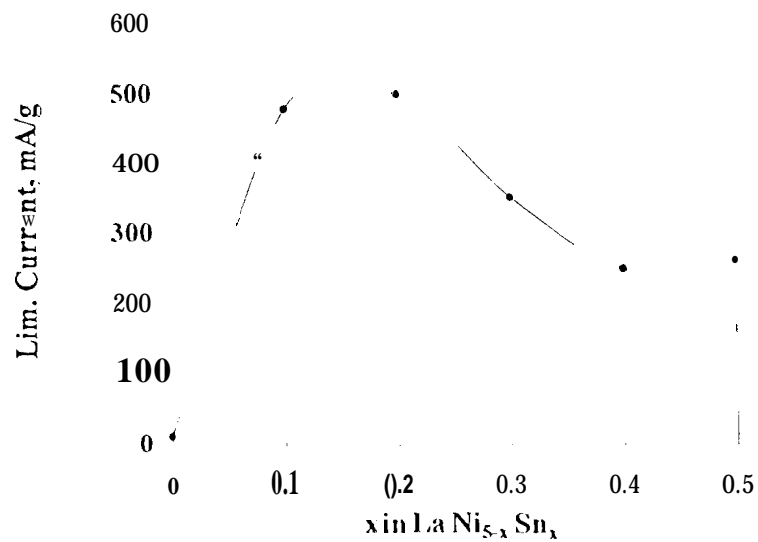


Fig. 2: Diffusion limiting currents of  $\text{LaNi}_{5-x}\text{Sn}_x$  alloys, estimated from potentiodynamic polarization curves



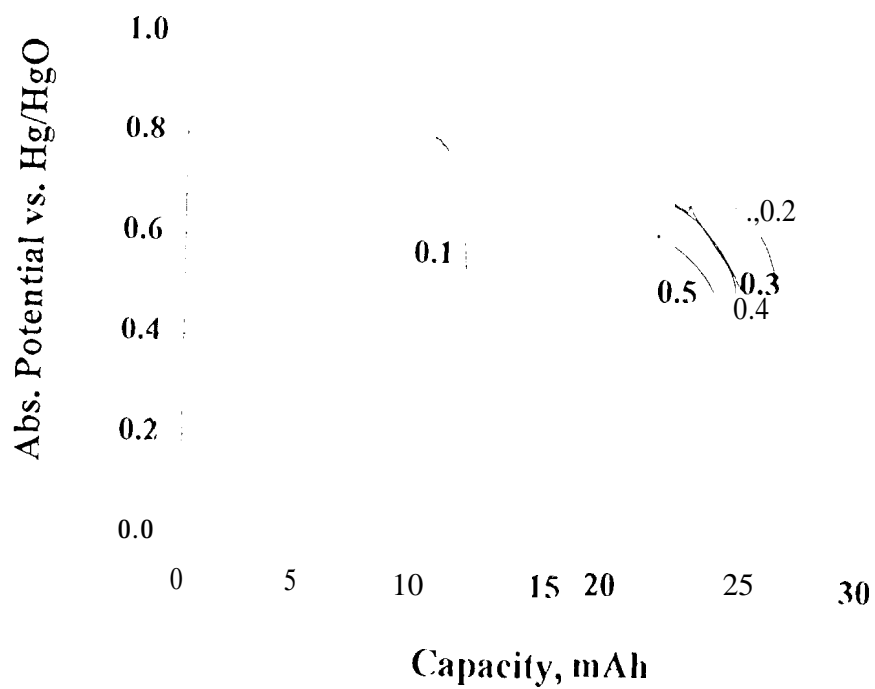


Fig.3. Discharge curves of LaNi<sub>5-x</sub>Sn<sub>x</sub> alloys,

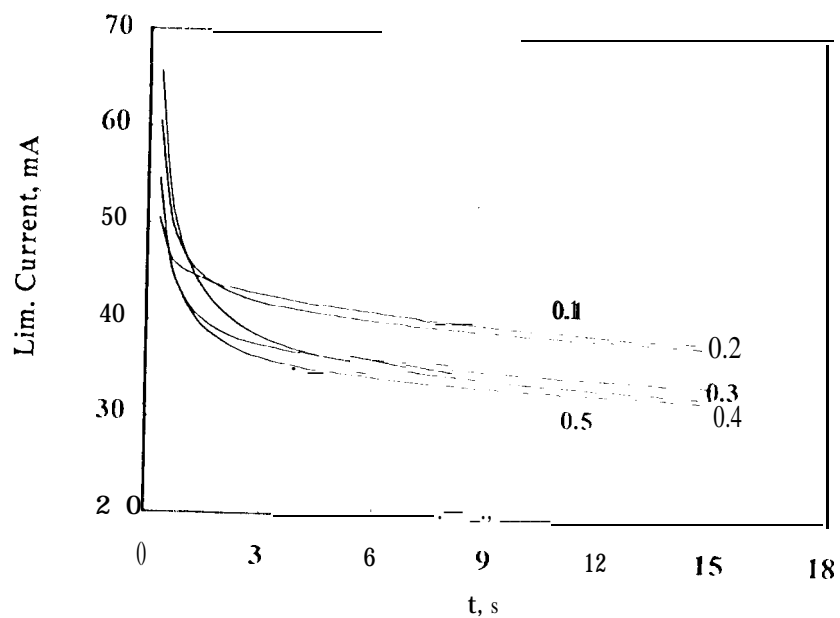


Fig 4 : Chronoamperometric curves of LaNi<sub>5-x</sub>Sn<sub>x</sub> alloys at a potentiostatic pulse of +400 mV vs OCV.

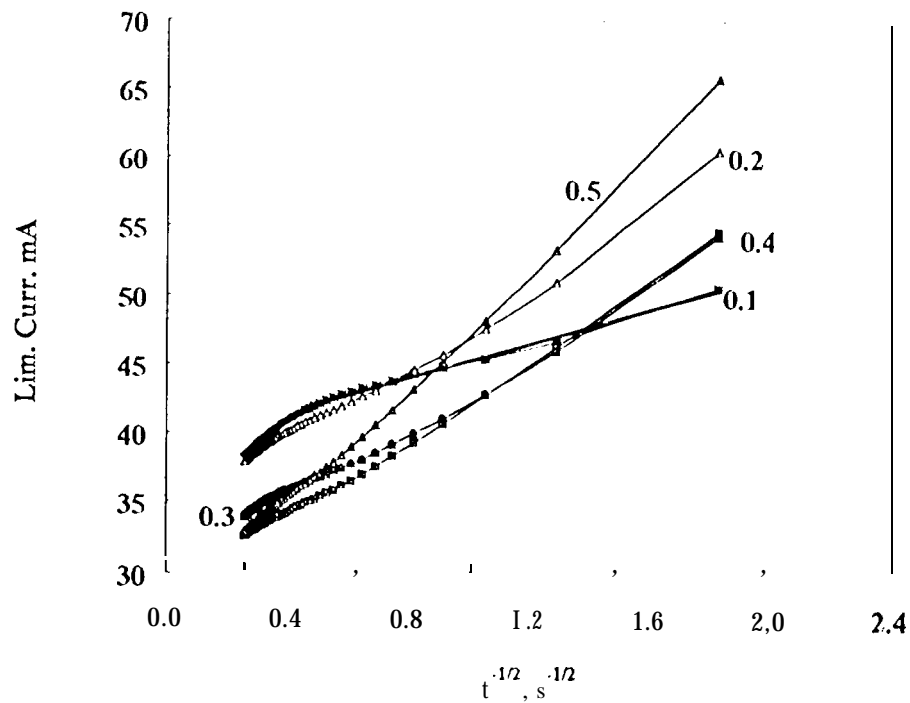


Fig. 5: Analyses of chronoamperometric curves of  $\text{LaNi}_{5-x}\text{Sn}_x$  alloys, recast from Fig. 4.

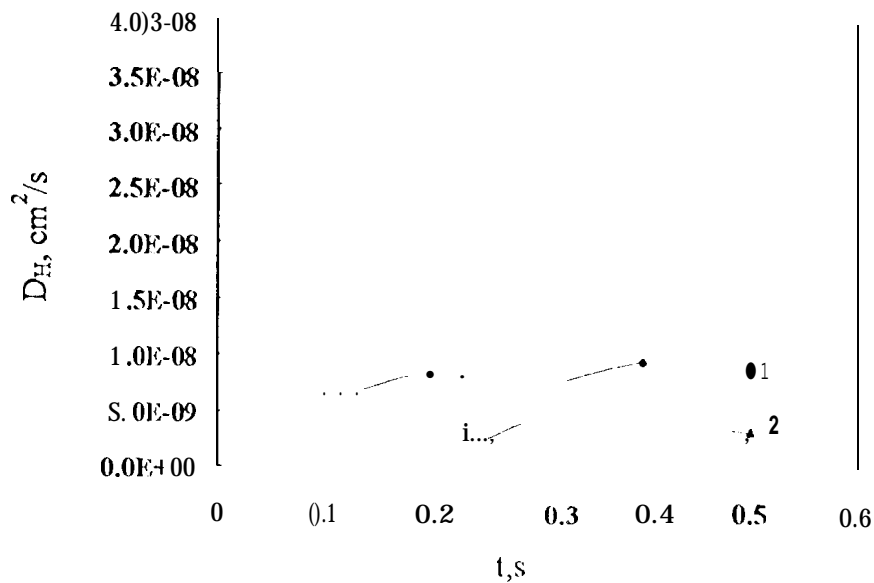


Fig. 6: Variation of diffusion coefficient of hydrogen in Sn-modified  $\text{LaNi}_5$  alloys with the Sn content by 1) Chronoamperometry and 2) Chronocoulometry.

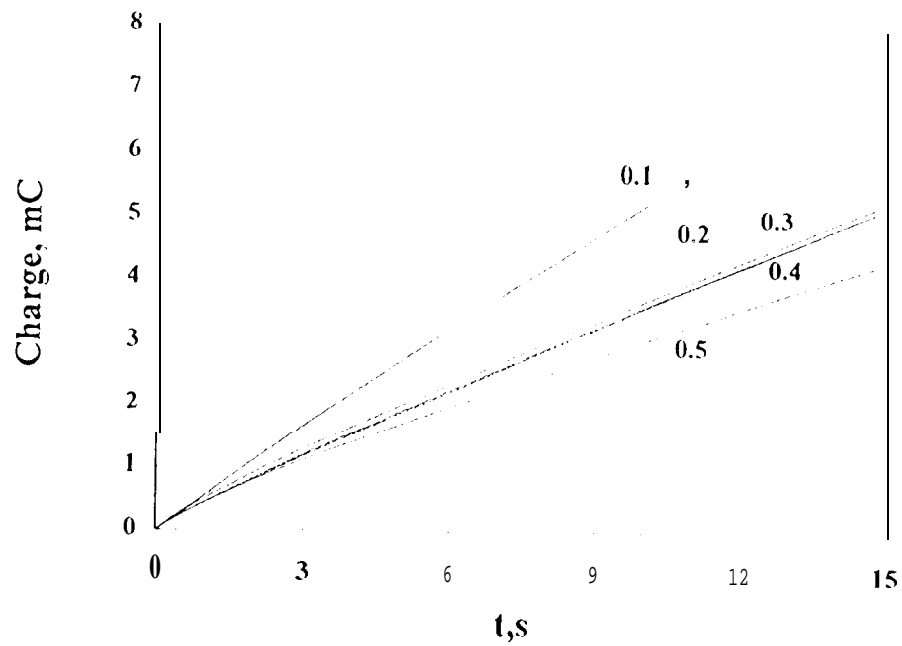


Fig. 7 : Chronocoulometric curves of  $\text{LaNi}_{5-x}\text{Sn}_x$  alloys

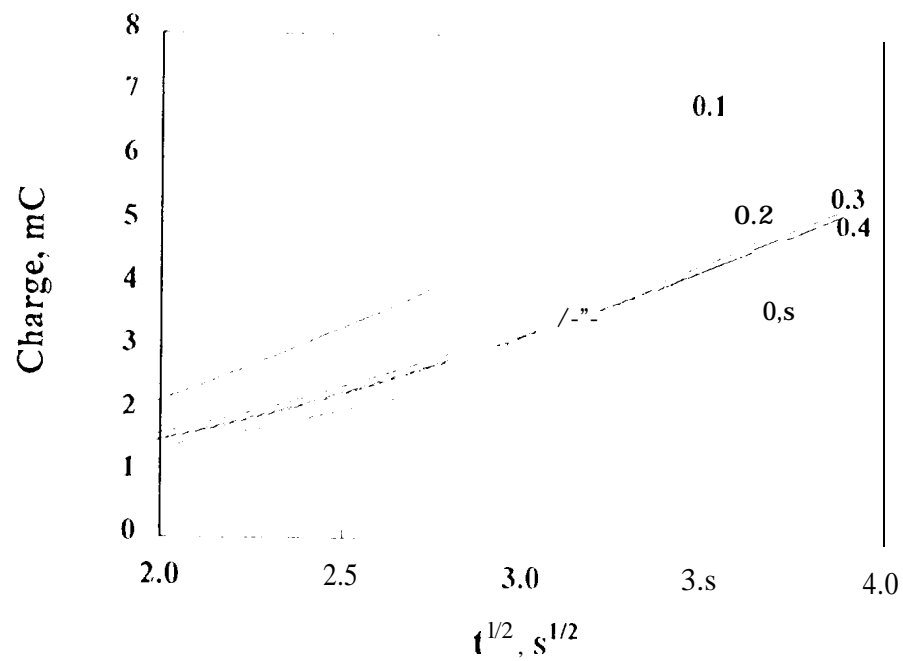


Fig. 8 : Analyses of chronocoulometric response of  $\text{LaNi}_{5-x}\text{Sn}_x$  alloys, recast from Fig. 7

Table 1: Diffusion coefficients of  $\text{LaNi}_{5-x}\text{Sn}_x$  MH alloys by chronoamperometric and chronocoulometric methods

$x$ in $\text{LaNi}_{5-x}\text{Sn}_x$	Capacity mAh/g	Concen., $C_H$ m. mol/cc	Chronoamp. $\text{mA}\cdot\text{s}^{-1/2}$	Chronocoul. $\text{mC}\cdot\text{s}^{-1/2}$	$D_H$ (Chronamp) $\text{cm}^2/\text{s}$	$D_H$ (Chronocoul.) $\text{cm}^2/\text{s}$
0.1	141	2.19	6.2	28.8	$6.69 \times 10^{-9}$	$3.6 \times 10^{-8}$
0.2	285	4.59	14.5	1.97	$8.38 \times 10^{-9}$	$3.85 \times 10^{-9}$
0.3	253	3.97	11.9	19.5	$7.53 \times 10^{-9}$	$4.27 \times 10^{-9}$
0.4	271	4.28	14.4	19.5	$9.36 \times 10^{-9}$	$4.31 \times 10^{-9}$
0.5	249	3.82	12.6	15.6	$9.03 \times 10^{-9}$	$3.23 \times 10^{-9}$